Appendix B: Host-parasite population model

Population model equations

The model consists of 14 partial-differential equations describing state variables for the number of moving and stationary calves, yearlings, and adults (N_C, N_Y, N_A) and the total numbers of within-host parasites (adult parasites P, developing larvae L_4 and arresting larvae L_{4A}) in both moving and stationary adult hosts, and pre-infective and infective parasite stages in the environment (L_0, L_3). Variables corresponding to **moving hosts** are denoted with a hat and written in black (e.g., $\widehat{N}_C$), whereas variables corresponding to **stationary hosts** have no hat and are in blue (e.g., N_C). Model equations are below, and parameter descriptions and assumed values are given in Table B1.

Host population

The equations for the change in moving and stationary calves ($\widehat{N}_C$, N_C), yearlings ($\widehat{N}_Y$, N_Y), and adult ($\widehat{N}_A$, N_A) caribou hosts are:

$$\frac{\partial \widehat{N}_C}{\partial t} - c_s \frac{\partial \widehat{N}_C}{\partial x} = \underbrace{-\mu_C \widehat{N}_C}_{\substack{\text{natural}\\ \text{mortality}}} \underbrace{-\theta(t)\,\widehat{N}_C}_{\text{stopping}} \underbrace{+\omega(t)\,N_C}_{\text{starting}} \tag{B1}$$

$$\frac{\partial N_C}{\partial t} = \underbrace{-\mu_C N_C}_{\substack{\text{natural}\\ \text{mortality}}} \underbrace{+\theta(t)\,\widehat{N}_C}_{\text{stopping}} \underbrace{-\omega(t)\,N_C}_{\text{starting}} \tag{B2}$$

$$\frac{\partial \widehat{N}_Y}{\partial t} - c_s \frac{\partial \widehat{N}_Y}{\partial x} = -\mu_Y \widehat{N}_Y - \theta(t)\,\widehat{N}_Y + \omega(t)\,N_Y \tag{B3}$$

$$\frac{\partial N_Y}{\partial t} = -\mu_Y N_Y + \theta(t)\,\widehat{N}_Y - \omega(t)\,N_Y \tag{B4}$$

$$\frac{\partial \widehat{N}_A}{\partial t} - c_s \frac{\partial \widehat{N}_A}{\partial x} = \mu_A \widehat{N}_A - \theta(t)\,\widehat{N}_A + \omega(t)\,N_A \tag{B5}$$

$$\frac{\partial N_A}{\partial t} = -\mu_A N_A + \theta(t)\,\widehat{N}_A - \omega(t)\,N_A \tag{B6}$$

At the start of the breeding season, after spring migration, there is an instantaneous shift in the population up one age class as new calves are born, calves become yearlings, and yearlings are added to the adult population. New calves are added at the start of breeding season depending on the number of adult female caribou that survived to arrive at the breeding grounds and the per-capita rate of successful calf production.

The only way in which parasites affected host population dynamics in our model was by depressing the rate of successful calf production in spring. Calf production depends on parasite burdens according to the relationship from Stien et al. (2002b):

$$p\big(\bar{P}(t)\big) = p_0\left(1 - \frac{1}{1+\exp\big(a - b\,\bar{P}(t)\big)}\right), \tag{B7}$$

where p_0 is the probability of having a calf in a given year (or, equivalently, the average proportion of adult female caribou that successfully produce a calf) in the absence of parasitism, *a* and *b* are parameters that control the shape of the curve, and $\bar{P}(t)$ is the average parasite burden τ_b days prior to calving. Specifically, we calculated $\bar{P}(t)$ as:

$$\bar{P}(t) = \frac{\int_x \left(P(x,\ t-\tau_b) + \hat{P}(x,\ t-\tau_b)\right) dx}{\int_x \left(N_A(x,\ t-\tau_b) + \widehat{N_A}(x,\ t-\tau_b)\right) dx}. \tag{B8}$$

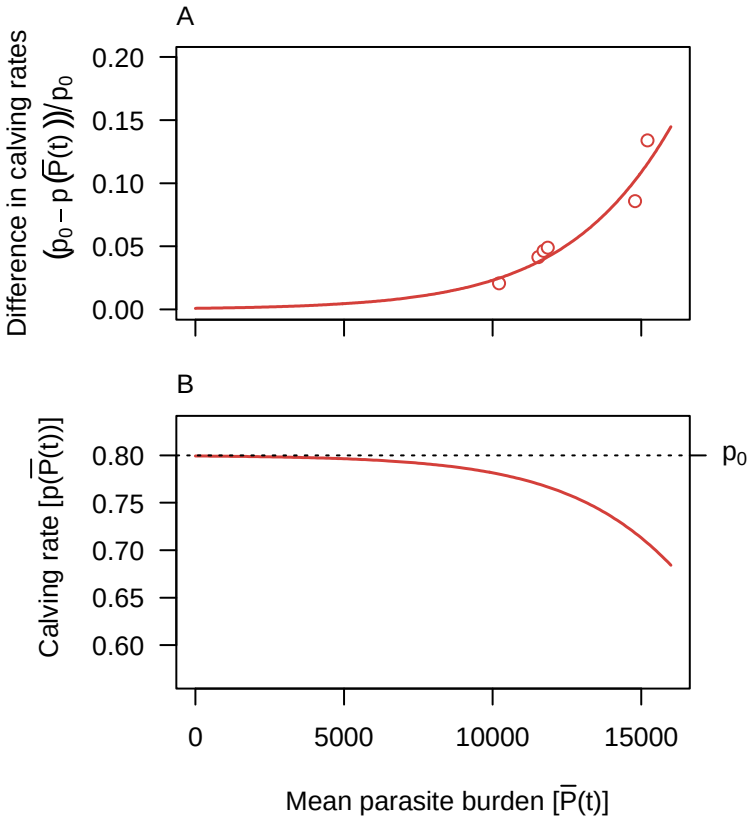

Figure B1. A. The relationship between the difference in calving rates between treated and untreated female reindeer as a function of mean parasite burden of untreated female reindeer that were culled in October, from Stien et al. (2002b). Treated female reindeer received an antihelminth that was effective against infections of *O. gruehneri.* B. The transformed relationship from A, giving the calving rate as a function of mean parasite burden (red) with a baseline calving rate of 0.8 yr^{-1}.

We ignore parasite burdens in calves and yearlings, as surveys indicate low prevalence and intensity of infection in these age classes that are unlikely to affect the population dynamics of either host or parasite (Hoar 2012).

Within-host parasites

We consider three separate stages of within-host parasites: arresting larvae L_{4A}, developing larvae L_4, and adult parasites P. Each of these stages is modelled separately in moving and stationary hosts. The equations are:

$$\frac{\partial \hat{L}_{4A}}{\partial t} - c_s \frac{\partial \hat{L}_{4A}}{\partial x} = \underbrace{\beta\, \chi(t)\, L_3 \hat{N}_A}_{\substack{\text{attachment} \\ \text{and arresting}}} \underbrace{- (\mu_A + \mu_4)\hat{L}_{4A}}_{\text{mortality}} \underbrace{- \theta(t)\, \hat{L}_{4A}}_{\substack{\text{host} \\ \text{stops}}} \underbrace{+ \omega(t)\, L_{4A}}_{\substack{\text{host} \\ \text{starts}}} \quad \text{(B9)}$$

$$\frac{\partial L_{4A}}{\partial t} = \beta\, \chi(t)\, L_3 N_A - (\mu_A + \mu_4) L_{4A} + \theta(t)\, \hat{L}_{4A} - \omega(t)\, L_{4A} \quad \text{(B10)}$$

$$\frac{\partial \hat{L}_4}{\partial t} - c_s \frac{\partial \hat{L}_4}{\partial x} = \underbrace{\beta\big(1 - \chi(t)\big) L_3 \hat{N}_A}_{\substack{\text{attachment} \\ \text{and developing}}} \underbrace{- (\mu_A + \mu_4)\hat{L}_4}_{\text{mortality}} \underbrace{- \rho_4 \hat{L}_4}_{\text{development}} \underbrace{- \theta(t)\, \hat{L}_4}_{\substack{\text{host} \\ \text{stops}}} \underbrace{+ \omega(t)\, L_4}_{\substack{\text{host} \\ \text{starts}}} \quad \text{(B11)}$$

$$\frac{\partial L_4}{\partial t} = \beta(1 - \chi(t))\, L_3 N_A - (\mu_A + \mu_4) L_4 - \rho_4 L_4 + \theta(t)\, \hat{L}_4 - \omega(t)\, L_4 \quad \text{(B12)}$$

$$\frac{\partial \hat{P}}{\partial t} - c_s \frac{\partial \hat{P}}{\partial x} = \rho_4 \hat{L}_4 - \left(\underbrace{\mu_A + \mu_P + \nu_P \left(\frac{\hat{P}}{\hat{N}_A} \frac{(k+1)}{k} + 1 \right)}_{\substack{\text{density-dependent} \\ \text{parasite mortality}}} \right) \hat{P} \underbrace{- \theta(t)\, \hat{P}}_{\substack{\text{host} \\ \text{stops}}} \underbrace{+ \omega(t)\, P}_{\substack{\text{host} \\ \text{starts}}} \quad \text{(B13)}$$

$$\frac{\partial P}{\partial t} = \rho_4 L_4 - \left(\mu_A + \mu_P + \nu_P \left(\frac{P}{N_A} \frac{(k+1)}{k} + 1 \right) \right) P + \theta(t)\, \hat{P} - \omega(t)\, P \quad \text{(B14)}$$

Each host ingests larvae at per parasite rate β (d^{-1}) and the parameter $\chi(t)$ controls the proportion of ingested larvae that enter the arrested state. The uptake rate β is unknown and difficult to estimate for free-ranging wildlife, so we tested the sensitivity of model outputs to three different magnitudes of β (Table B1). As described in the main text, mortality and development rates were borrowed from studies of closely related species, as estimates specific to *O. gruehneri* were not available.

Free-living parasite stages

We modelled pre-infective and infective stages of larvae separately. The pre-infective stage included eggs, L1 larvae, and L2 larvae, as was done in the analysis of the experiment data. The equations for change in pre-infective and infective larvae are:

$$\frac{\partial L_0}{\partial t} = \underbrace{\lambda(t)\left(P^{1+\gamma}N_A + \widehat{P^{1+\gamma}N_A}\right)}_{\substack{\text{Shedding of eggs} \\ \text{into the environment}}} \underbrace{-\mu_0(T(t))L_0}_{\text{mortality}} \underbrace{-\rho_0(T(t))\,L_0}_{\text{development}} \quad \text{(B15)}$$

$$\frac{\partial L_3}{\partial t} = \underbrace{\rho_0(T(t))\,L_0}_{\substack{\text{development} \\ \text{from L0}}} \underbrace{-\mu_3(T(t))L_3}_{\text{mortality}} \underbrace{-\beta L_3(N_A + \widehat{N_A})}_{\substack{\text{uptake by} \\ \text{hosts}}} \quad \text{(B16)}$$

Terms in red include the mortality rates of pre-infective and infective stages and the development rate of pre-infective stages to infective L3. These terms were modelled as functions of temperature, $T(t)$, according to the MTE relationships parameterized from experiments (Appendix A; see Table A5 for final estimates applied in the population model).

The shedding rate of eggs into the environment varied throughout the year according to the relationships described by Stien et al. (2002a). Briefly, shedding rates depend on (1) the density-independent rate at which adult parasites produce eggs, $\lambda(t)$, which is a function of day-of-year, (2) the negative impact of increasing infection intensity on individual parasite fecundity (density dependence, γ) and (3) the fecal production rate of caribou hosts (included in $\lambda(t)$), which is a function of day-of-year (representing seasonal differences in food availability). These effects combine to result in the shedding rates illustrated in Figure B2.

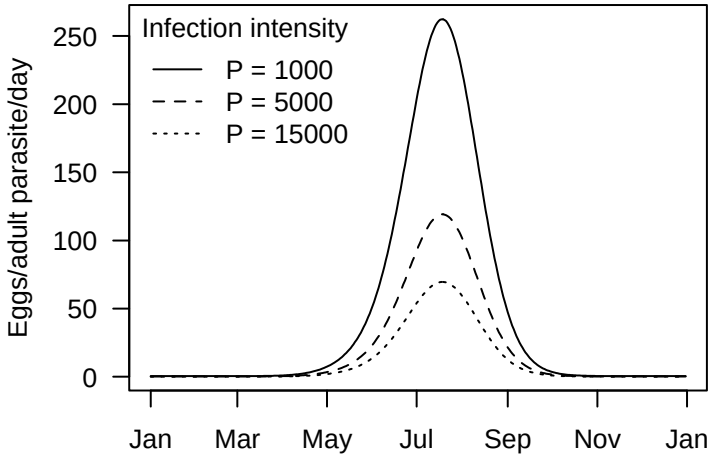

Figure B2. Estimated average output of eggs per adult O. gruehneri per day, as estimated by Stien et al. (2002a) and applied in our population model.

Parameterization

Table B1. Parameter descriptions and assumed values used in model simulations.

Symbol	**Description**	**Value**
μ_C	Daily per-capita mortality rate of calves, calculated from annual survival reported in Boulanger et al. (2011)	(1 – 0.45)/365 d^{-1}
μ_Y	Daily per-capita mortality rate of yearlings, calculated from annual survival reported in Boulanger et al. (2011)	(1 – 0.86)/365 d^{-1}
μ_A	Daily per-capita mortality rate of adult caribou, calculated from annual survival reported in Boulanger et al. (2011)	(1 – 0.86)/365 d^{-1}
$\theta(t)$	Rate of host stopping per day	Variable (Figure B3)
$\omega(t)$	Rate of host starting per day	Variable (Figure B3)
p_0	Per-capita rate of calf production in the absence of parasites (Boulanger et al. 2011)	0.8 yr^{-1}
a	Parameters controlling the decline in calf production with increasing mean parasite burden, as estimated by Stien et al. (2002b)	7.025
b		0.000328 $(parasite)^{-1}$

τ_b	Number of days prior to calving when parasite burdens are assumed to affect calving rates, based on the relationship from Stien et al. (2002b)	240 days
c_s	The movement speed of caribou during migration, based on collar data (Gunn et al. 2001)	14 km d^{-1}
μ_P	Density independent mortality rate of within-host adult parasites, based on *Ostertagia ostertagi* (Grenfell et al. 1987)	0.1713 d^{-1}
ν_P	Per-parasite increase in natural adult parasite mortality, based on the density-dependent mortality of *Ostertagia ostertagi* (Grenfell et al. 1987)	0.3082×10^{-6} $parasite^{-1}$ d^{-1}
$\chi(t)$	The proportion of ingested larvae that undergo arrested development	Varied in four different scenarios (Figure 3)
μ_4	Mortality rate of ingested L4, based on *Ostertagia ostertagi* (Grenfell et al. 1987)	0.002 d^{-1}
ρ_4	Development rate of (developing) L4, based on *Ostertagia ostertagi* (Grenfell et al. 1987)	0.06 d^{-1}
β	The rate at which a hosts ingests infective L3 (i.e., transmission rate)	low: 10^{-7} $L3^{-1}$ d^{-1} base: 10^{-6} $L3^{-1}$ d^{-1} high: 10^{-5} $L3^{-1}$ d^{-1}
$\lambda(t)$	Egg output per adult worm per day in the absence of density dependence (Figure B2) (Stien et al. 2002b)	Variable
γ	Strength of density dependence in egg production rate ($\gamma < 1$ yields lower per-parasite fecundity at high parasite burdens) (Stien et al. 2002b)	-0.49
q_{NB}	Aggregation parameter for the negative binomial distribution of parasites among hosts, estimated from surveys of *Ostertagia gruehneri* in Bathurst caribou (Hoar 2012)	0.994

Host starting and stopping

To capture aggregation of hosts in key times throughout the annual cycle, we assumed temporal and spatial variability in starting and stopping rates as illustrated in Figure B3. These values were chosen to reproduce a typical annual cycle of aggregation during calving and breeding periods, but were not fitted to any particular dataset.

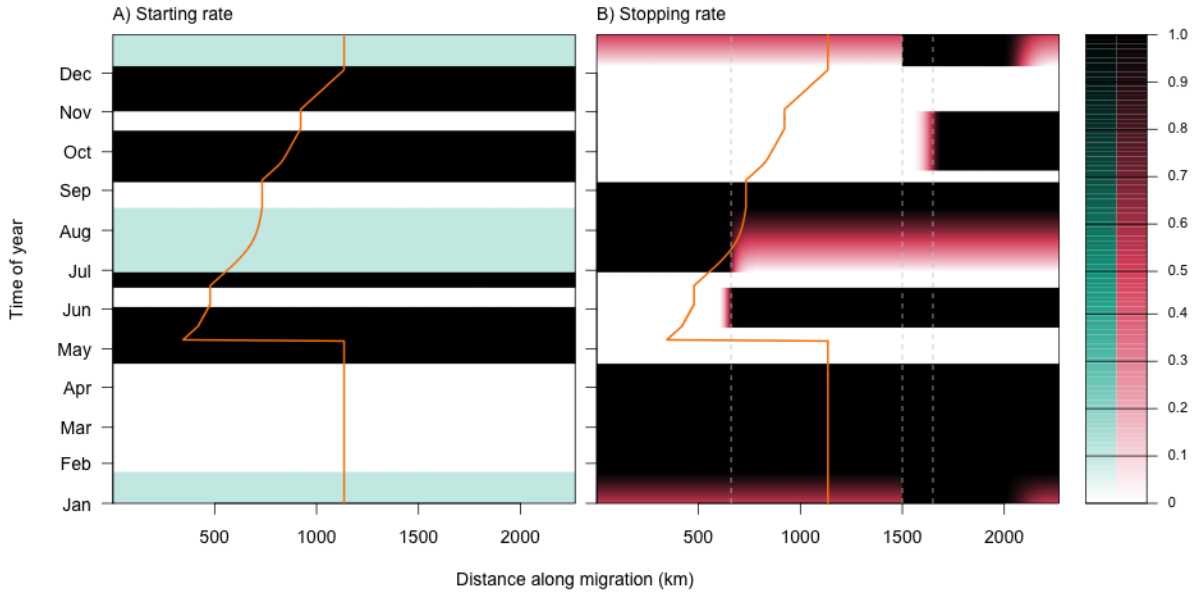

Figure B3. The spatiotemporal distribution of assumed rates of host starting and stopping (d^{-1}) were chosen to capture aggregation on the calving grounds (~660 km) and during the fall breeding season (~1650 km) and dispersal over the summer range in July and August and overwinter in December through April 20th. Along the x-axis is the distance along the 1-D migration corridor (km), with x = 0 km corresponding to the winter range. Along the y-axis is the day of year, from January 1 (bottom) to December 31 (top). Starting and stopping rates are shaded from 0 d^{-1} (white), meaning no starting or stopping, to 1 d^{-1} (black), meaning all animals are started or stopped at that place and time. At intermediate rates, a proportion of the population will stop and/or start with each daily timestep. The orange line shows the location of the leading edge of the host population on each day-of-year, with the corresponding starting and stopping rates for that location shown in Figure B4.

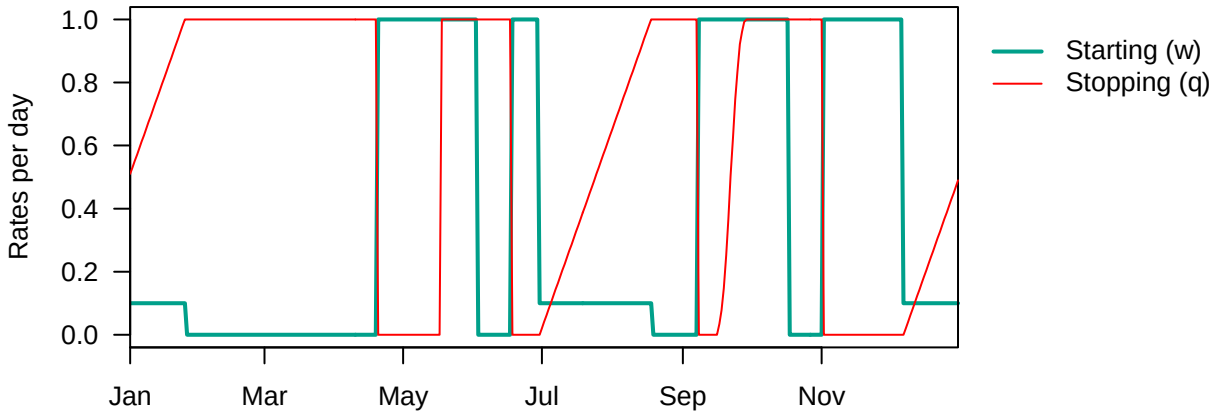

Figure B4 . Rate of starting and stopping per day over an annual cycle for the leadding edge of the host population on each day (orange line shown in Figure B3).

Results

Sensitivity to transmission rate, β

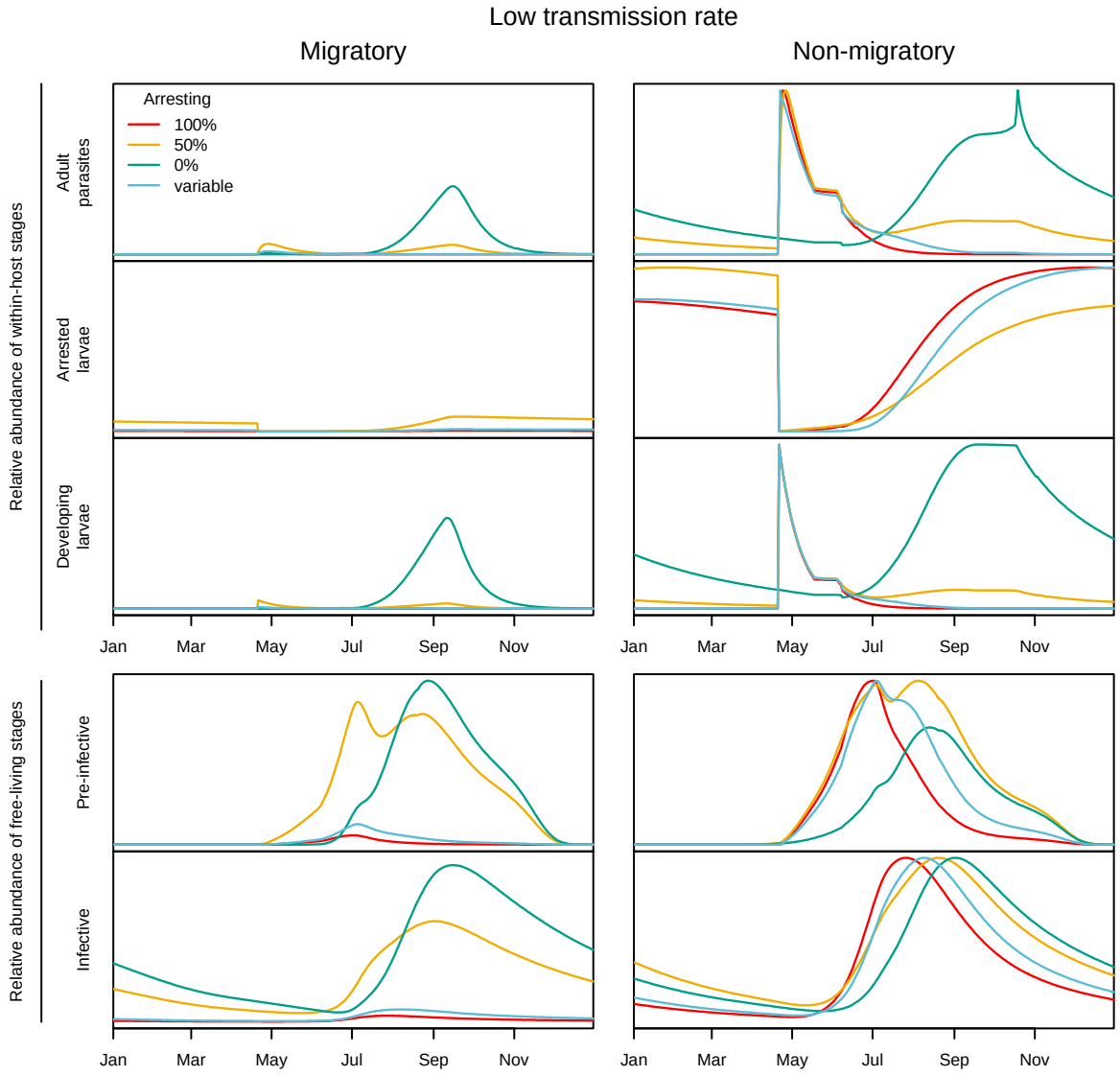

Figure B5. (Figure 6 under low parasite transmission rate.) The relative abundance of parasites between simulations with migratory and non-migratory hosts (i.e., abundance scaled to the maximum parasites *within each arresting scenario*) over the last year of a 30-year simulation, assuming low transmission of $\beta = 10^{-7}$ d^{-1}. Simulations including migration (left) or not (right) are shown, each under four scenarios for larval arrested development (colours; see legend).

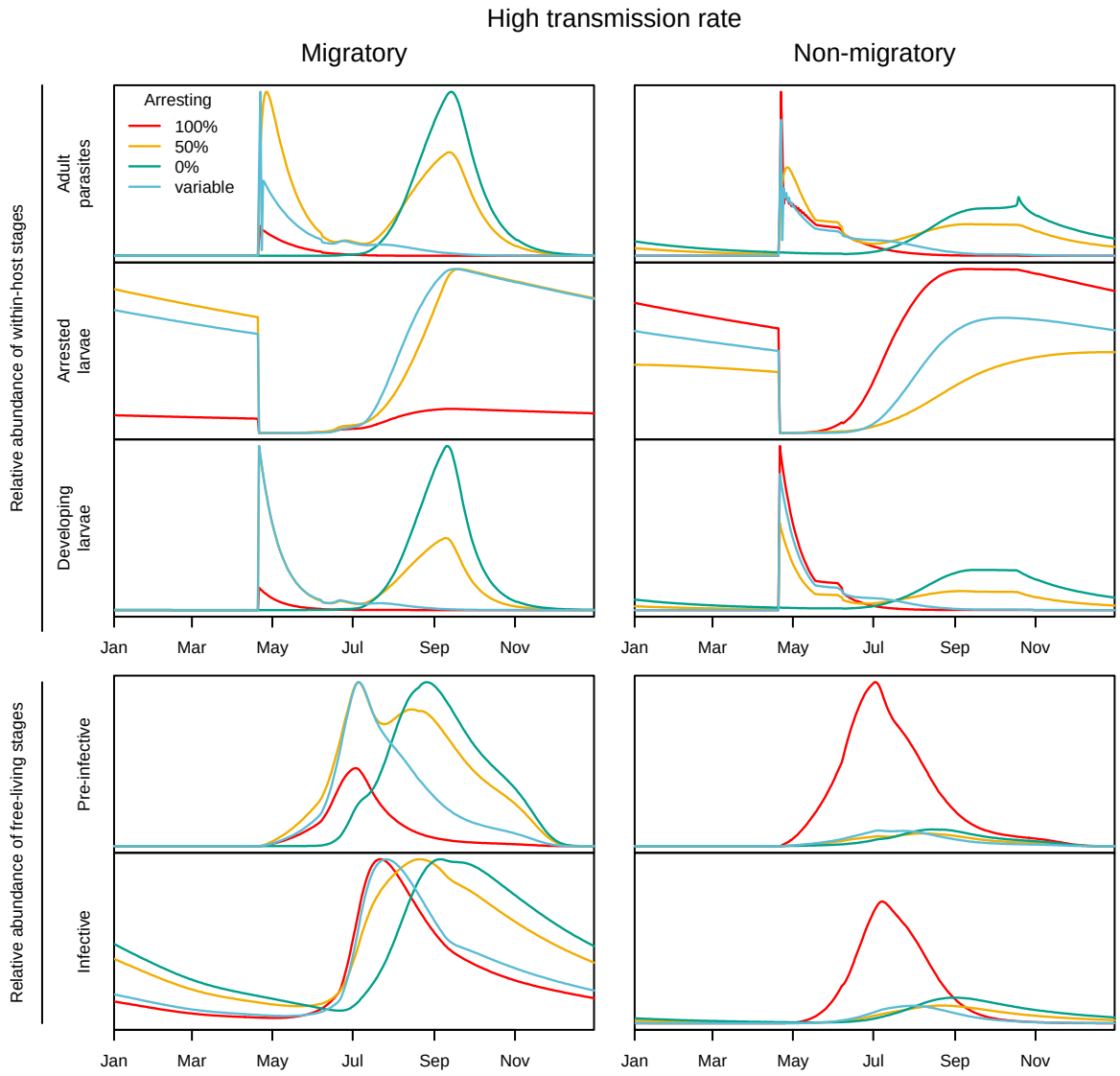

Figure B6. (Figure 6 under high parasite transmission rate.) The relative abundance of parasites between simulations with migratory and non-migratory hosts (i.e., abundance scaled to the maximum parasites *within each arresting scenario*) over the last year of a 30-year simulation, assuming high transmission of $\beta = 10^{-5}$ d^{-1}. Simulations including migration (left) or not (right) are shown, each under four scenarios for larval arrested development (colours; see legend).

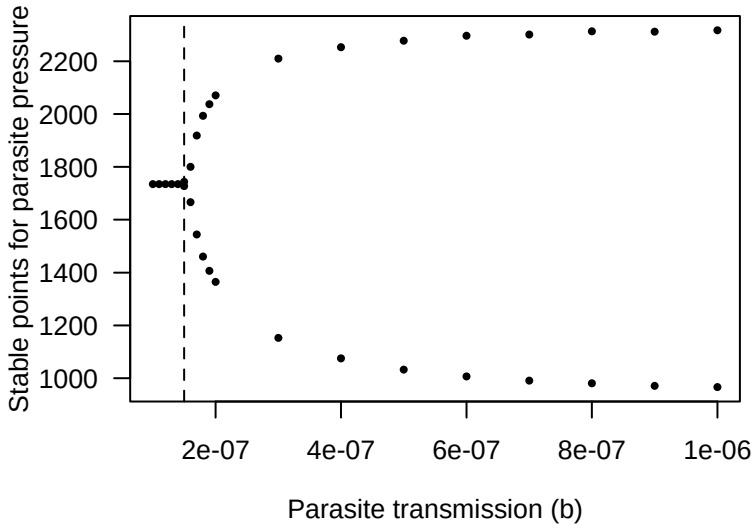

Figure B7. Bifurcation diagram showing a Hopf bifurcation at a parasite transmission rate of $\beta \approx 1.5 \times 10^{-7}$ where the system transitions from a single stable point to a two-point limit cycle under the 100% arresting scenario.

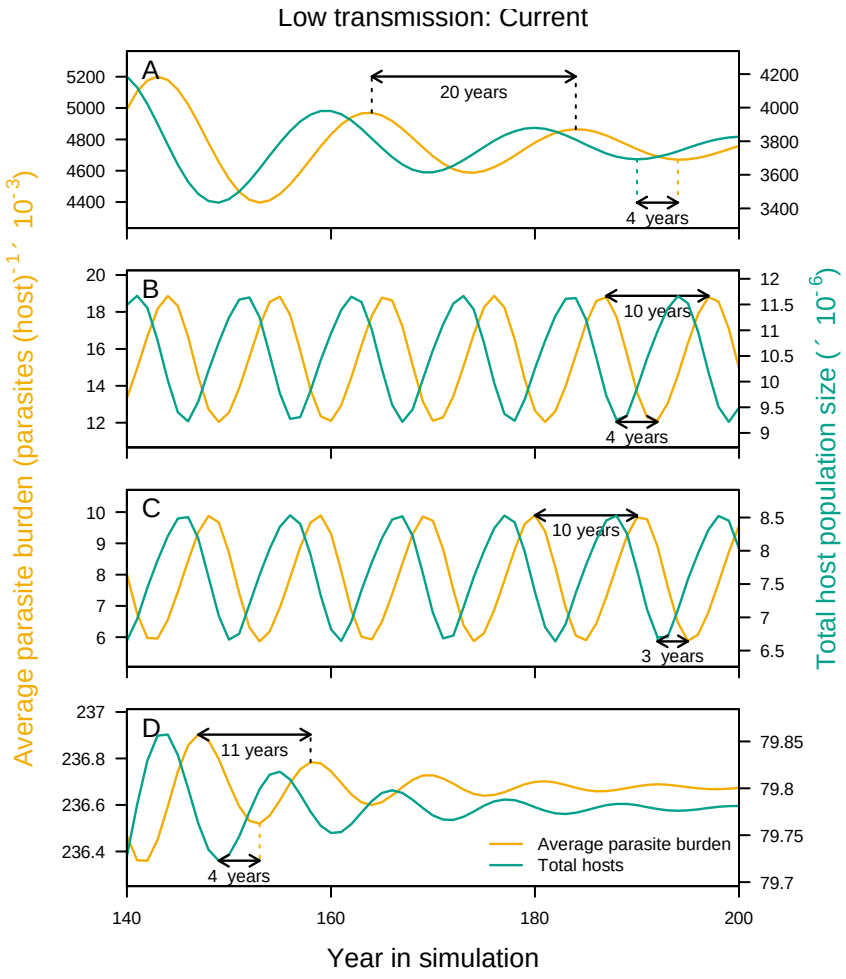

Figure B8. (Figure 7 under **low parasite transmission** ($\beta = 10^{-7}$ d^{-1}).) Cycles in the annual parasite burden (calculated as the sum of the daily mean adult parasite burdens across all hosts divided by 365 days; yellow) and the total host population (sum of stationary and moving adults, yearlings, and calves on June 8th each year; turquoise) for years 140 to 200 under four scenarios for larval arrested development: (A) scenario 1: 100% arresting, (B) scenario 2: 50% arresting, (C) scenario 3: 0% arresting, and (D) scenario 4: variable arresting.

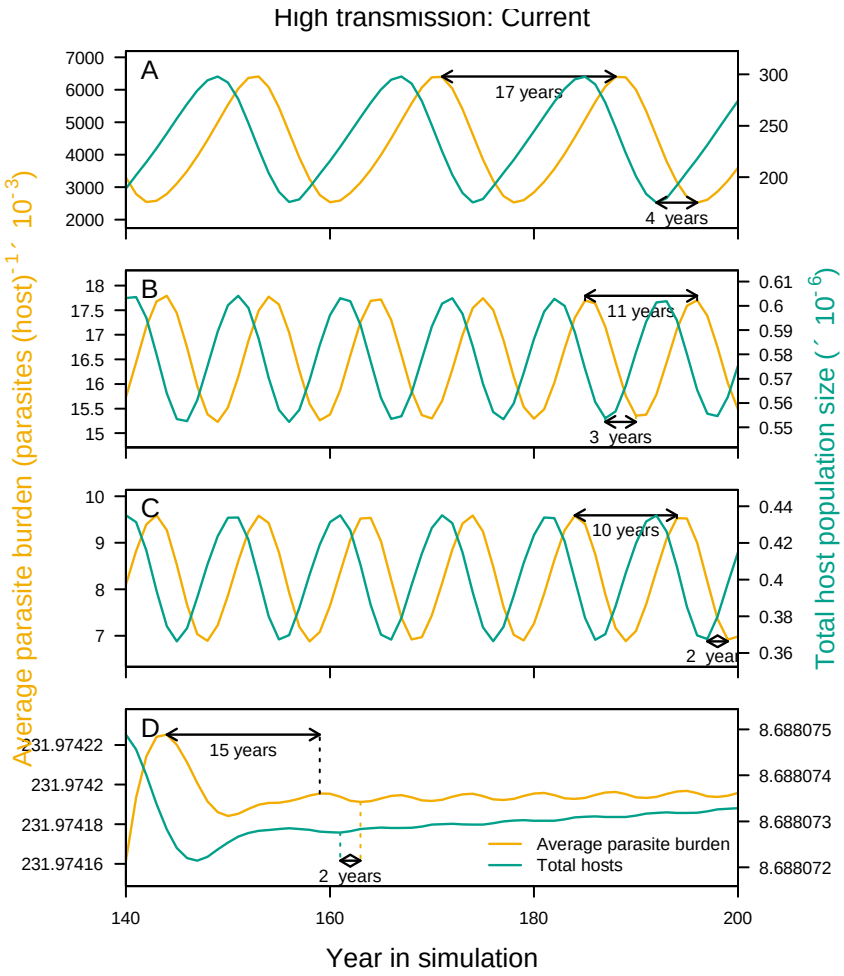

Figure B9. (Figure 7 under h**igh parasite transmission** ($\beta = 10^{-5}$ d^{-1}).) Cycles in the annual parasite burden (calculated as the sum of the daily mean adult parasite burdens across all hosts divided by 365 days; yellow) and the total host population (sum of stationary and moving adults, yearlings, and calves on June 8th each year; turquoise) for years 140 to 200 under four scenarios for larval arrested development: (A) scenario 1: 100% arresting, (B) scenario 2: 50% arresting, (C) scenario 3: 0% arresting, and (D) scenario 4: variable arresting.

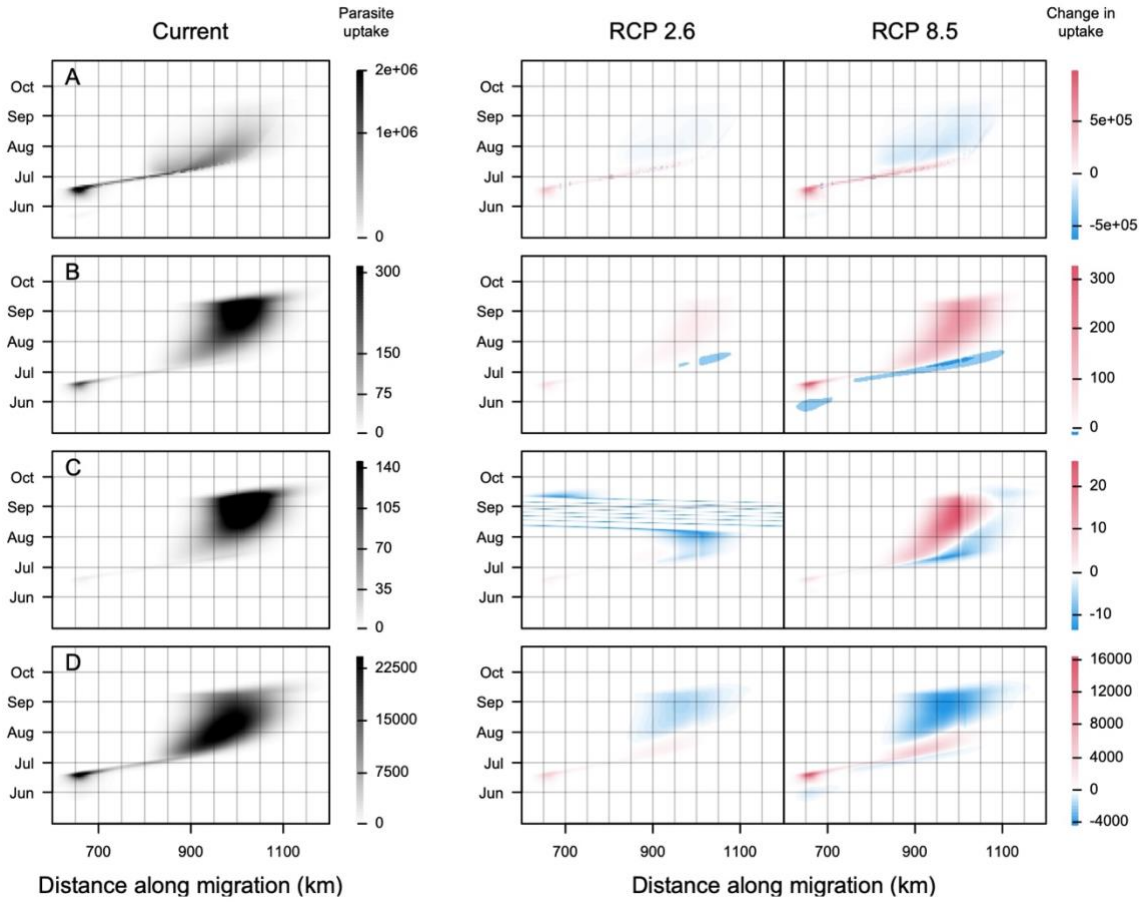

Figure B10. Parasite uptake rate per host (left) and the change in uptake from the current climate under RCP 2.6 and RCP 8.5 emissions scenarios in over space (x-axis) and day-of-year for year 200 of simulations (y-axis). Axes are truncated to focus on the period of transmission. Rows A-D show uptake under the four scenarios for arrested development (A = 100%, B = 50%, C = 0%, D = variable).

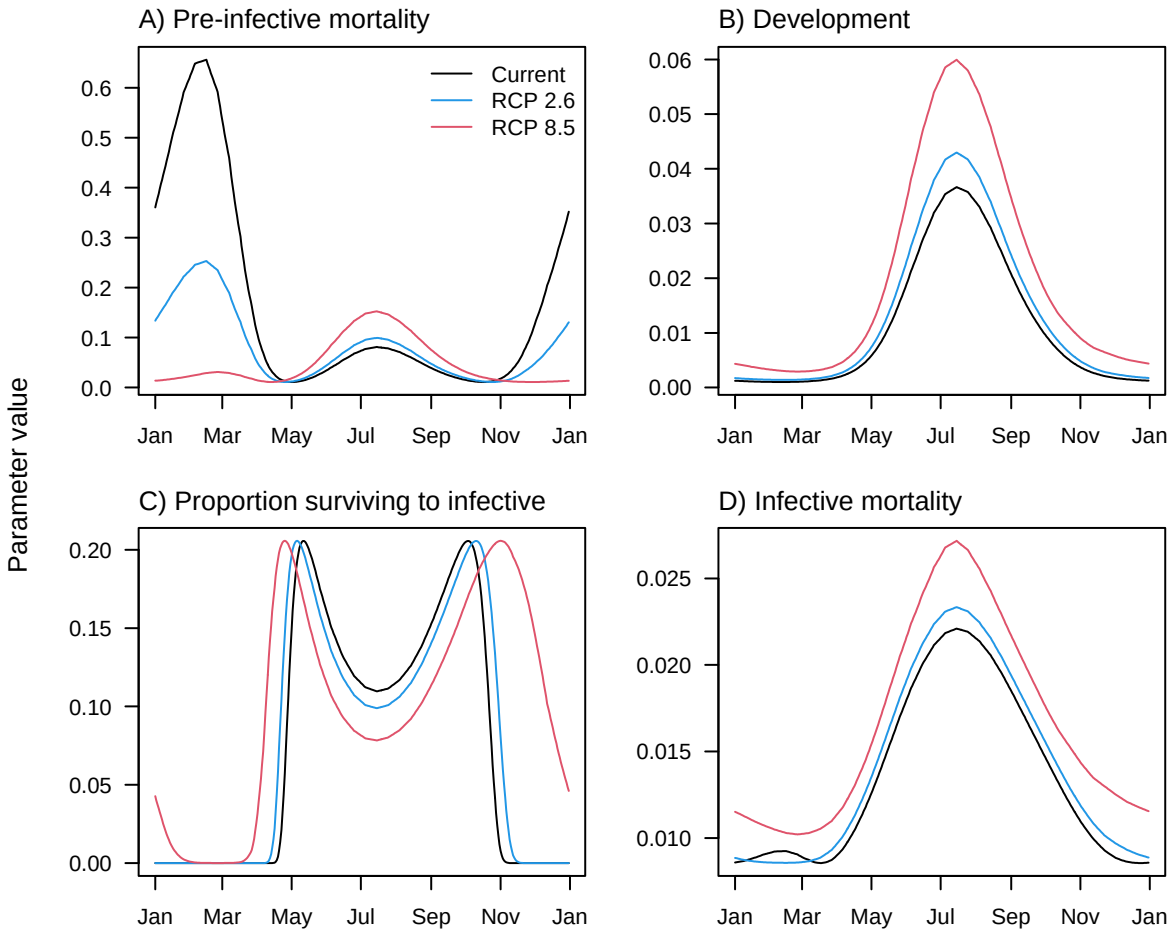

134

135 Figure B11. Projected (A) pre-infective mortality rate per day - μ_0, (B) development rate per day -ρ_0, (C) the
136 proportion of eggs surviving to L3 (infective), calculated as $\exp\left(-\mu_0\left(\frac{1}{\rho_0}\right)\right)$, and (D) the infective mortality per day
137 - μ_3 under current temperatures and future climate with RCP 2.6 and RCP 8.5 emissions scenarios.

138

References

Boulanger, J., Gunn, A., Adamczewski, J., and Croft, B. 2011. A data-driven demographic model to explore the decline of the Bathurst caribou herd. J. Wildl. Manage. **75**(4): 883–896. doi:10.1002/jwmg.108.

Grenfell, B.T., Smith, G., and Anderson, R.M. 1987. A mathematical model of the population biology of Ostertagia ostertagi in calves and yearlings. Parasitology **95**(January 2016): 389–406. doi:10.1017/S0031182000057826.

Gunn, A., Dragon, J., and Boulanger, J. 2001. Seasonal movements of satellite-collared caribou from the Bathurst herd. Final Rep. to West Kitikmeot Slave Study Soc. Yellowknife, NWT **80**.

Hoar, B.M. 2012. Ecology and Transmission Dynamics of Ostertagia gruehneri in Barrenground Caribou. Available from https://prism.ucalgary.ca/handle/11023/289.

Stien, A., Irvine, R.J., Langvatn, R., Albon, S.D., and Halvorsen, O. 2002a. The population dynamics of Ostertagia gruehneri in reindeer: A model for the seasonal and intensity dependent variation in nematode fecundity. Int. J. Parasitol. **32**(8): 991–996. doi:10.1016/S0020-7519(02)00071-1.

Stien, A., Irvine, R.J., Ropstad, E., Halvorsen, O., Langvatn, R., and Albon, S.D. 2002b. The impact of gastrointestinal nematodes on wild reindeer: experimental and cross-sectional studies. J. Anim. Ecol. **71**: 937–945.